Quantum-Mechanical Calculation of the Third Virial Coefficient of He^4†*

SIGURD YVES LARSEN‡
Columbia University, New York, New York
(Received 17 December 1962)

Using the method of binary collisions, the third virial coefficient of He^4 at low temperatures is calculated for a potential consisting of an attractive square well and a repulsive core. The shape of this potential is chosen so as to optimize the fit of the second virial coefficient with experimental data. From a comparison of the results with the third virial data the existence of a three-body bound state is inferred. A binding energy of 0.26°K, calculated from the potential, brings the adjusted results and the experimental data into agreement.

INTRODUCTION

THE equation of state of a dilute gas may conveniently be written as

$$pV=NkT(1+B/V+C/V^2\cdots),$$

where B and C are the second and third virial coefficients, respectively. These coefficients, and higher ones, have been calculated classically for a number of gases and a variety of binary potentials.[1]

Our interest lies with He^4, and for such a light gas, at low temperatures, the quantum-mechanical deviations from the classical behavior are really important. A correct treatment must, therefore, be developed within the quantum-mechanical framework. Such a method for the calculation of the second virial coefficient was derived by Uhlenbeck and Beth,[2] and by Gropper,[3] in the 1930's, and subsequently has been used by Massey and Buckingham,[4] de Boer and Michels,[5] and others.[6] It was only comparatively recently, however, when Lee and Yang developed their binary collisions method,[7] that a systematic procedure of calculating the higher coefficients became available. The first study of the third virial coefficient using this technique was that of Pais and Uhlenbeck[8] who have considered $C(T)$ for several limiting cases, including that characterized by strongly bound two- and three-body states.

In this work we seek to determine $C(T)$ at low temperatures by evaluating terms in a binary collisions expansion for the third virial coefficient of He^4. We assume a definite potential and calculate exactly the corresponding two-body kernels, in terms of which we carry out the expansion. The potential used has a finite, though very high, repulsive core together with an attractive square well. This potential was chosen because it possesses the essential characteristics of the true potential while being of such a form that the two-body wave functions are expressible analytically. The associated parameters are determined through a study of the second virial coefficient, and a fitting to the experimental data at high and low temperatures.

For simplicity, and since it is not known whether or not He^4 has a very weak two-body bound state,[9] we assume that this is not the case. We admit no two-body bound states in our calculation.

The numerical evaluation of the binary collisions expressions for $T=1.7, 4$, and 8° K yield results which are positive and increase as the temperature decreases. This is in sharp contrast with the experimental behavior of the third virial which decreases with decreasing temperature, becoming negative at about 4° K.

We, then, consider a three-body bound state and find that by including its contribution we are able to bring theory and experiment into agreement. The value of the binding energy, 0.26° K, was obtained from an approximate calculation using our potential.

FUGACITY EXPANSION

The pressure and the density of a Boltzmann gas may be expressed as expansions in the fugacity z

$$P/kT=\sum_1^\infty b_l z^l, \tag{1}$$

$$N/\Omega=\sum_1^\infty l b_l z^l, \tag{2}$$

where

$$b_l=(\Omega l!)^{-1}\int\langle X_1\cdots X_l|\,U_l\,|X_1\cdots X_l\rangle d^3X_1\cdots d^3X_l \tag{3}$$

becomes volume-independent when we let the volume

† This work has been supported in part by the U. S. Atomic Energy Commission and in part by Pfister fellowships.
* Submitted in partial fulfillment of the requirement for the degree of Doctor of Philosophy in the Faculty of Pure Science, Columbia University.
‡ Present address: National Bureau of Standards, Washington, D. C.
[1] A very small sampling is: J. de Boer and A. Michels, Physica **6**, 97 (1939); J. S. Rowlinson, J. Chem. Phys. **19**, 287 (1951); R. J. Lunbeck and C. A. ten Seldam, Physica **17**, 788 (1951).
[2] G. E. Uhlenbeck and E. Beth, Physica **3**, 729 (1936); E. Beth and G. E. Uhlenbeck, *ibid.* **4**, 915 (1937).
[3] L. Gropper, Phys. Rev. **50**, 963 (1936); **51**, 1108 (1937).
[4] H. S. Massey and R. A. Buckingham, Proc. Roy. Soc. (London) **A168**, 378 (1938); **A169**, 205 (1939).
[5] J. de Boer and A. Michels, Physica **6**, 409 (1939).
[6] R. A. Buckingham, J. Hamilton, and H. S. Massey, Proc. Roy. Soc. (London) **A179**, 103 (1941); J. E. Kilpatrick, W. E. Keller, E. F. Hammel, and N. Metropolis, Phys. Rev. **94**, 1103 (1954); J. E. Kilpatrick, W. E. Keller, and E. F. Hammel, *ibid.* **97**, 9 (1955).
[7] T. D. Lee and C. N. Yang, Phys. Rev. **105**, 1119 (1957); **113**, 1165 (1959).
[8] A. Pais and G. E. Uhlenbeck, Phys. Rev. **116**, 250 (1959).
[9] J. E. Kilpatrick, W. E. Keller, and E. F. Hammel, Phys. Rev. **97**, 9 (1955).

Ω become large. We shall always take this to be the case. If H_N is the Hamiltonian for N particles and

$$W_N \equiv \exp(-H_N/kT), \tag{4}$$

then the U_l functions are defined by

$$\begin{aligned}
&\langle 1'|W_1|1\rangle = \langle 1'|U_1|1\rangle,\\
&\langle 1',2'|W_2|1,2\rangle = \langle 1'|U_1|1\rangle\langle 2'|U_1|2\rangle + \langle 1',2'|U_2|1,2\rangle,\\
&\langle 1',2',3'|W_3|1,2,3\rangle = \langle 1'|U_1|1\rangle\langle 2'|U_1|2\rangle\\
&\quad\times\langle 3'|U_1|3\rangle + \langle 1'|U_1|1\rangle\langle 2',3'|U_2|2,3\rangle + \langle 2'|U_1|2\rangle\\
&\quad\times\langle 1',3'|U_2|1,3\rangle + \langle 3'|U_1|3\rangle\langle 1',2'|U_2|1,2\rangle\\
&\qquad + \langle 1',2',3'|U_3|1,2,3\rangle, \text{ etc.}
\end{aligned} \tag{5}$$

This is a procedure that was first introduced by Ursell[10] and by Mayer[11] for classical statistical mechanics and by Kahn and Uhlenbeck[12] for quantum statistical mechanics. We see that U_l requires us to be able to solve the l-body problem. Furthermore, in the case of a Bose gas and symmetric statistics we are interested in b_l^s and U_l^s.

These problems have been treated by Lee and Yang who have shown how to calculate U_l^s in terms of U_l, and how to obtain U_l, for $l>2$, in terms of U_2.[7]

We are concerned with the calculation of U_1, U_2, U_3 and their symmetric counterparts. Knowing b_1^s, b_2^s, b_3^s, we may, then, combine equations similar to Eqs. (1) and (2) to obtain

$$pV = NkT\{1-(v_0b_2^s)z-[2(v_0b_3^s)-2(v_0b_2^s)^2]z^2\cdots\}. \tag{6}$$

We have also used the fact that $b_1 = b_1^s = v_0^{-1}$, and have let

$$v_0 = (2\pi\hbar^2/mkT)^{3/2} = \lambda_T^3,$$

where λ_T is the thermal wavelength.

Writing z as a power series in the density,

$$z = v_0(N/\Omega) - 2v_0^3b_2^s(N/\Omega)^2\cdots, \tag{7}$$

we may now substitute for z in Eq. (6) to obtain

$$pV = NkT\left[1-\frac{v_0(v_0b_2^s)N}{\Omega} - \frac{[2(v_0b_3^s)-4(v_0b_2^s)^2]N^2v_0^2}{\Omega^2}\cdots\right]. \tag{8}$$

Comparing this with the usual expansion for the equation of state, we find that the second virial coefficient is

$$B = -Nb_2^sv_0^2, \tag{9}$$

and the third virial coefficient is

$$\begin{aligned}
&C = -N^2v_0^2[2(v_0b_3^s)-4(v_0b_2^s)^2],\\
&C = -2N^2v_0^3b_3^s + 4B^2.
\end{aligned} \tag{10}$$

[10] H. D. Ursell, Proc. Cambridge Phil. Soc. **23**, 685 (1927).
[11] J. E. Mayer, J. Chem. Phys. **5**, 67 (1937); J. E. Mayer and P. G. Ackerman, *ibid.* **5**, 74 (1937); J. E. Mayer and S. F. Harrison, *ibid.* **6**, 87 (1938); S. F. Harrison and J. E. Mayer, *ibid.* **6**, 101 (1938).
[12] B. Kahn and G. E. Uhlenbeck, Physica **5**, 399 (1938).

SECOND VIRIAL COEFFICIENT

At high temperatures the second virial is given correctly by the classical expression:

$$B = 2\pi N\int_0^\infty \{1-\exp[-V(r)/kT]\}r^2dr \tag{11}$$

while at low temperatures we use an expression first derived by Beth and Uhlenbeck,[2] and by Gropper[3]

$$\begin{aligned}
B = &-N(4\pi\hbar^2/2mk)^{3/2}T^{-3/2}2^{-5/2}\\
&-16\pi^{1/2}N(\hbar^2/mkT)^{5/2}\sum_{\substack{l=0\\ \text{even}}}^{\infty}(2l+1)\\
&\times\int_0^\infty \exp[-(\hbar^2/mkT)y^2]\delta_l(y)ydy,
\end{aligned} \tag{12}$$

where the first term of the equation represents the contribution to the virial from a free Bose gas, and $\delta_l(y)$ is the lth phase shift. Consistent with our intentions of not allowing bound states, we have not included contributions from discrete energy levels.

The experimental data which we seek to fit with Eqs. (11) and (12) are quite old, and may be found, sifted and weighed, in Keesom's book "Helium"[13] published in 1942. We have used his table of "Adopted values of second and third virial coefficients for helium," as well as values given in his later paper with Kistemaker.[14]

We found especially useful a formula given in this latter paper which fits the second virial coefficient data from 1.8 to 60° K. Expressed in units of cm^3/mole, instead of Amagat units, it reads

$$B = -(385.7)T^{-1} + 15.2 \tag{13}$$

with an estimated uncertainty of 5%.

Newer low-temperature data have been published by Keller[15] who reports on five isotherms (from 2.154 to 3.961° K), as well as reevaluates the isotherms of Keesom and Walstra.[16] In both these cases the resulting values for the second virial coefficient differ by less than 10% from the values given by Eq. (13).

No such agreement is to be found when we consider respective values for the third virial coefficient. Keller's results at 2.3° K, for example, differ by more than an order of magnitude from those of Kistemaker and Keesom. The determination of the third virial is, however, marginal at best, and the situation is best expressed by quoting Keesom[13]: "It is evident that the curves drawn in the figure are more or less arbitrary, and therefore rather uncertain. Nevertheless we estimate that the general course might be real, so C seems to

[13] W. H. Keesom, *Helium* (Elsevier Press, Amsterdam, Holland, 1942), p. 34.
[14] J. Kistemaker and W. H. Keesom, Physica **12**, 227 (1946).
[15] W. E. Keller, Phys. Rev. **97**, 1 (1955).
[16] W. H. Keesom and W. K. Walstra, Physica **7**, 985 (1940).

reach large negative values below 3° K⋯." We note that while at very low temperatures Keller's third virials are smaller in magnitude than Keesom's, they are also negative.

Our two-body potential has the following form

$$\begin{aligned} V(r)&=U, \quad 0<r<\sigma \\ &=-\epsilon, \quad \sigma<r<a \\ &=0, \quad a<r, \end{aligned} \tag{14}$$

where U is very large compared to ϵ. We seek parameters σ, a, ϵ, U which will fit the experimental second virial coefficient data of He^4 at high and low temperatures. We do not admit the case of a bound state.

In the next section we shall give an operator equation for U_2, and it will be seen that $U_2=0$ for $\beta=0$. We also give expressions for the matrix elements of U_2. In the case of an infinite repulsive core these expressions for the matrix elements will not go to zero when β goes to zero. (This is because when U is infinite there is an excluded volume, and the solutions of the two-body problem do not form a complete set of states for all space, implying that the sum

$$\sum_n \psi_n(r')\psi_n^*(r)$$

will not reduce to a δ function.) It is, then, convenient to choose U to be finite, though very high compared to the depth of the attractive well. The virials will not be very sensitive to the particular height chosen, although we must keep in mind that for finite U the onset of the bound state depends on the values of all the parameters. If we again let k equal Boltzmann's constant, then $U=10^6k$ ergs.

We now consider the high-temperature region, which determines σ. Helium gas behaves classically only at very high temperatures. Indeed, de Boer and Michels[17] have calculated the quantum-mechanical correction to a Lennard-Jones gas at 256° K and found them to be of the order of 5% of the classical answer. We shall, therefore, in "fitting," consider the very highest temperatures listed in Keesom's table of "adopted values," spanning a 200° K range from 373.15 to 573.15° K. Within this high-temperature range, and somewhat lower, the classical virial derived from our potential has the wrong shape and does not fit well the experimental data. A classical expression for B, suitably approximated for high temperatures, reads

$$B=(2\pi/3)N[\sigma^3-(a^3-\sigma^3)(n/T)], \tag{15}$$

where $(a^3-\sigma^3)>0$, (n/T) is small. B simply becomes larger and larger reaching an asymptote determined uniquely by the diameter of the repulsive core. The B experimental rises in value, reaches a maximum, and then decreases in magnitude, which is a behavior typical of that given by gases composed of "compressible" molecules. The optimum value for σ is 2.1 Å.

We use the data of the low-temperature region to determine the remaining parameters. For convenience we chose these to be n and $\mathbb{S}$, defined by

$$\begin{aligned} a-\sigma&=(\pi/2)(\hbar^2/mk)^{1/2}(\mathbb{S}/n)^{1/2}, \\ \epsilon&=nk, \end{aligned} \tag{16}$$

where k is Boltzmann's constant. Were U to be infinite, our constraint barring the existence of two-body bound states would be expressed as $\mathbb{S}<1$.

To obtain a good agreement between our expressions and experiment, it is necessary that $\mathbb{S}$ be near 1. Further, this agreement is rather insensitive to the particular value of n chosen, hence to the depth of the well. In other words, the second virial is not very sensitive to the details of the potential but responds to its strength, which in our case nearly admits a bound state. In fact, though we obtained the lowest residuals (best fit) for $\mathbb{S}=0.997$, $n=2$(°K), we were able to exhibit a fit nearly as good for $\mathbb{S}=0.96$ and $n=1$. The shapes of the two curves $B_{\text{exp}}(T)$ and $B_{\text{theor}}(T)$ are different. For the lowest temperature B_{theor} is larger in magnitude than B_{exp}, for the higher temperatures the converse is true (all the virials in the low-temperature calculation are negative). The best agreement and the smallest residuals is, then, obtained when we allow the two curves to cross over near the low-temperature end.

Theoretical and experimental values for the second virial coefficient are found in Table I. A detailed discussion of the fitting is found in Appendix A.

BINARY KERNELS FOR A BOLTZMANN GAS

We wish to evaluate the following two binary kernels[18]:

$$U_2(\beta)=\exp(-\beta H_2)-\exp(-\beta T), \tag{17}$$

$$X(\beta)=-V\exp(-\beta H_2)=\frac{\partial}{\partial\beta}U_2(\beta)+TU_2(\beta), \tag{18}$$

where H_2 is the Hamiltonian for two particles.

$$H_2=T+V=H_{\text{c.m.}}+H_{\text{rel}}, \quad \beta=1/kT. \tag{19}$$

$H_{\text{c.m.}}$ consists only of a kinetic energy term, and U_2 will factor into a product

$$\langle \mathbf{r}_1',\mathbf{r}_2'|\,U_2\,|\mathbf{r}_1,\mathbf{r}_2\rangle=\langle \mathbf{R}'|\,U_1\,|\mathbf{R}\rangle\langle \mathbf{r}'|\,U_2\,|\mathbf{r}\rangle, \tag{20}$$

in which

$$\mathbf{R}=\tfrac{1}{2}(\mathbf{r}_1+\mathbf{r}_2), \quad \mathbf{r}=\mathbf{r}_1-\mathbf{r}_2,$$

$$\begin{aligned} \langle \mathbf{R}'|\,U_1\,|\mathbf{R}\rangle&=\langle \mathbf{R}'|\exp(-\beta H_{\text{c.m.}})\,|\mathbf{R}\rangle \\ &=(m/\pi\hbar^2\beta)^{3/2}\exp[-(\mathbf{R}-\mathbf{R}')^2m/\hbar^2\beta], \end{aligned} \tag{21}$$

$$\begin{aligned} \langle \mathbf{r}'|\,U_2\,|\mathbf{r}\rangle&=\sum_n \psi_n(\mathbf{r}')\psi_n^*(\mathbf{r})\exp[-\beta(E_n)_{\text{rel}}] \\ &\quad-\sum_p \phi_p(\mathbf{r}')\phi_p^*(\mathbf{r})\exp[-\beta(E_p)_{\text{rel}}], \end{aligned} \tag{22}$$

[17] J. de Boer and A. Michels, Physica 5, 945 (1938).

[18] T. D. Lee and C. N. Yang, Phys. Rev. 113, 1165 (1959).

TABLE I. Comparison between experimental and theoretical values of the second virial coefficient for the optimum shape of our potential ($S=0.997$, $n=2.0$, $U=10^6k$, $\sigma=2.1$ Å). Theoretical values at low temperatures are obtained from an equation involving phase shifts, while at high temperatures the classical expressions are used. B's are expressed in units of cc/mole.

T (°K)	B_{exp}				B_{theor}[e]
	Keesom[a]	Keller[b]	Keller[c]	K&W, re-ev.[d]	
1.7	−211.6				−223.4
2.154		−176.4	−159.3		
2.2	−160.1				−162.7
2.324		−175.7	−140.8		
2.610				−123.8	
2.7	−127.6				−126.0
2.862		−123.6	−117.8		
3.105				−108.3	
3.2	−105.3				−101.9
3.348		−103.4	−102.4		
3.7	−89.0				−83.7
3.721				−85.2	
3.961		−83.70	−83.31		
4.2	−76.9				−70.7
4.245				−78.25	
4.7	−66.9				−60.0
5.2	−58.9				−51.6
5.7	−52.4				−44.9
6.2	−47.0				−39.4
6.7	−42.3				−34.6
7.2	−38.3				−30.4
7.7	−34.8				−26.9
8.2	−31.8				−23.9
373.15	11.0				10.28
473.15	10.6				10.58
573.15	10.1				10.77

[a] The low-temperature values are obtained from the formula $B=-(385.7)T^{-1}+15.2$ proposed by Kistemaker and Keesom. The high-temperature values are taken from Keesom's *Helium*.
[b] Two-constant analysis.
[c] Three-constant analysis.
[d] Three-constant re-evaluation of the data of Keesom and Walstra by Keller.
[e] The theoretical values have been fitted to the data of Keesom.

where the ψ_n's are the energy eigenfunctions of H_{rel} and the ϕ_p's are the corresponding solutions of the free-relative Hamiltonian. Taking advantage of the fact that our potential is central and that we restrict ourselves to continuous solutions we may replace ψ_n by ψ_{ylm}, where

$$\psi_{ylm}=(2\pi^{-1})^{1/2}r^{-1}R_{yl}(r)Y_{lm}(\theta,\phi),$$
$$H_{rel}\psi_{ylm}=(\hbar^2/m)y^2\psi_{ylm}, \tag{23}$$

and

$$R_{yl}\rightarrow\sin[yr-l\pi/2+\delta_l(y)] \quad \text{as} \quad r\rightarrow\infty.$$

We proceed similarly for the ϕ's, noting that they have the same asymptotic form as that of the ψ's, except that their phase shifts $\delta_l(y)$ are zero.

We now wish to obtain U_2 in the momentum representation. If we let

$$F_l(kr)=(kr)j_l(kr),$$

where

$$j_l(kr)=(\pi/2kr)^{1/2}J_{l+\frac{1}{2}}(kr)$$

is a spherical Bessel function, and we define

$$\mathbf{K}=\mathbf{k}_1+\mathbf{k}_2, \quad \mathbf{k}=\tfrac{1}{2}(\mathbf{k}_1-\mathbf{k}_2),$$

then the matrix elements of U_2 are

$$\langle\mathbf{k}_1',\mathbf{k}_2'|U_2|\mathbf{k}_1,\mathbf{k}_2\rangle$$
$$=(2\pi)^{-3}\delta(\mathbf{K}-\mathbf{K}')\exp(-K^2\hbar^2\beta/4m)$$
$$\times 8(kk')^{-1}\sum_{l=0}(2l+1)P_l(\cos\Theta)$$
$$\times\int_0^\infty dy\int_0^\infty dr\int_0^\infty dr'\,F_l(kr)F_l(kr')$$
$$\times[R_{yl}(r')R_{yl}^*(r)]\exp(-\hbar^2\beta y^2/m), \tag{24}$$

where $P_l(\cos\Theta)$ is a Legendre polynomial and

$$\cos\Theta=\hat{k}\cdot\hat{k}', \quad [RR^*]=RR^*-(RR^*)_{free}.$$

We could now substitute in Eq. (24) the radial wave function obtained by solving the Schrödinger equation for our potential. This proves to be very cumbersome indeed and we seek a handier alternative.[19]

Consider the following Green's function:

$$\Gamma_y^l(r,r')=(2/\pi)P\int_0^\infty dk\,F_l(kr)F_l(kr')(k^2-y^2)^{-1}, \tag{25}$$

where P denotes the principal value of the integral. Then,

$$\phi_y^l(r)=F_l(yr)-\int_0^\infty\Gamma_y^l(r,r')[mV(r')/\hbar^2]\phi_y^l(r')dr' \tag{26}$$

satisfies

$$\left(\frac{d^2}{dr^2}+y^2-\frac{l(l+1)}{r^2}\right)\phi_y^l(r)=(m/\hbar^2)V(r)\phi_y^l(r), \tag{27}$$

which is the differential equation satisfied by the radial function R for given angular momentum l. $\phi_y^l(r)$ may be written as

$$\phi_y^l(r)=F_l(yr)+(2/\pi)P\int_0^\infty dk$$
$$\times F_l(kr)k\langle k|A_l|y\rangle(k^2-y^2)^{-1}, \tag{28}$$

where

$$k\langle k|A_l|y\rangle=-(m/\hbar^2)\int_0^\infty dr'\,F_l(kr')V(r')\phi_y^l(r'). \tag{29}$$

We state that the following expression for R_{yl},

$$R_{yl}(r)=\cos\delta_l(y)\Big(F_l(yr)+(2/\pi)P\int_0^\infty dz$$
$$\times F_l(zr)z\langle z|A_l|y\rangle(z^2-y^2)^{-1}\Big) \tag{30}$$

has the correct asymptotic behavior, i.e.,

$$R_{yl}\rightarrow\sin[yr-l\pi/2+\delta_l(y)] \quad \text{as} \quad r\rightarrow\infty. \tag{31}$$

[19] I am indebted to Dr. Franz Mohling for suggesting this approach and acquainting me with theorems concerning the A matrix.

We may now express U_2 in terms of the A matrix defined by Eq. (29). Substituting our new expression for $R_{yl}(r)$ and $R_{yl}(r')$ into $\langle \mathbf{k}_1', \mathbf{k}_2' | U_2 | \mathbf{k}_1, \mathbf{k}_2 \rangle$, and using

$$\int_0^\infty F_l(kr) F_l(yr) dr = (\pi/2)\delta(k-y), \tag{32}$$

$$P(x)^{-1}P(y)^{-1} = (y-x)^{-1}[P(x)^{-1} - P(y)^{-1}] + \pi^2 \delta(x)\delta(y), \tag{33}$$

$$\langle k | A_l | k \rangle = \tan\delta_l(k), \tag{34}$$

we obtain

$$\langle \mathbf{k}_1', \mathbf{k}_2' | U_2 | \mathbf{k}_1, \mathbf{k}_2 \rangle = (2\pi)^{-3}\delta(\mathbf{K}-\mathbf{K}') \exp(-K^2\hbar^2\beta/4m) \sum_{l=0}^{\infty} (2l+1) P_l(\cos\Theta)$$
$$\times \Big\{ 4\pi[kk'(k^2-k'^2)]^{-1}[\cos^2\delta_l(k') k \langle k | A_l | k' \rangle \exp(-\hbar^2\beta k'^2/m) - \cos^2\delta_l(k) k' \langle k' | A_l | k \rangle \exp(-\hbar^2\beta k^2/m)]$$
$$- 8(k^2-k'^2)^{-1} \int_0^\infty dy \, \langle k' | A_l | y \rangle \langle k | A_l | y \rangle \cos^2\delta_l(y) [P(k^2-y^2)^{-1} - P(k'^2-y^2)^{-1}] \exp(-\hbar^2\beta y^2/m) \Big\}. \tag{35}$$

Using Eq. (18) we determine the matrix elements of X from those of U_2:

$$\langle \mathbf{k}_1', \mathbf{k}_2' | X | \mathbf{k}_1, \mathbf{k}_2 \rangle = (2\pi)^{-3}\delta(\mathbf{K}-\mathbf{K}') \exp(-K^2\hbar^2\beta/4m)(\hbar^2/m) \sum_{l=0}^{\infty} (2l+1) P_l(\cos\Theta)$$
$$\times \Big\{ 4\pi(kk')^{-1} \cos^2\delta_l(k) k' \langle k' | A_l | k \rangle \exp(-\hbar^2\beta k^2/m) + 8 \int_0^\infty dy \, \langle k | A_l | y \rangle \langle k' | A_l | y \rangle \cos^2\delta_l(y)$$
$$\times P(k^2-y^2)^{-1} \exp(-\hbar^2\beta y^2/m) \Big\}. \tag{36}$$

Equations (35) and (36) together with the expression for the A matrix, given in Appendix B, represent a complete evaluation for our potential of the binary kernels U_2 and X. For the numerical work that ensues, however, we wish to eliminate all references to principal values. To this effect we rewrite integrals in the following way:

$$P\int_0^\infty dy \, f(y)(k^2-y^2)^{-1} = -P\int_0^\infty dy \, [f(k)-f(y)][k^2-y^2]^{-1} + f(k) P \int_0^\infty dy \, (k^2-y^2)^{-1} \tag{37}$$

but this last integral equals zero and the integrand of the remaining integral no longer requires us to take a principal value.

An analytical method of dealing with the limit $\mathbf{k}' \to \mathbf{k}$, $\mathbf{K}' \to \mathbf{K}$ is given in Appendix C.

EXPANSION OF U_3^s

We wish to calculate b_3^s. In order to do so, and following the prescriptions given by Lee and Yang in their paper,[7] we express the diagonal elements of U_3^s in terms of U_1, U_2, and U_3.

There is first the free-particle contribution which is obtained from terms in $U_1U_1U_1$ and is symbolically represented in Fig. 1. There are two diagrams and they both give the same result. Diagram (a) gives a contribution to b_3^s equal to

$$(3!\Omega)^{-1} \int U_1(\mathbf{k}_1,\mathbf{k}_3) U_1(\mathbf{k}_3,\mathbf{k}_2) U_1(\mathbf{k}_2,\mathbf{k}_1) d^3k_1 d^3k_2 d^3k_3 = (3^{3/2}6)^{-1}(mkT/2\pi\hbar^2)^{3/2}. \tag{38}$$

As diagram (b) gives the same answer, the total free contribution becomes

$$(b_3^s)_{\text{free}} = 3^{-5/2}(\lambda_T^3)^{-1}. \tag{39}$$

We shall then have terms in U_1U_2, one of which we represent by the diagram of Fig. 2. The contribution of this diagram to b_3^s is

$$(3!\Omega)^{-1} \int d^3k_1 d^3k_2 d^3k_3 \, U_2(\mathbf{k}_1,\mathbf{k}_3;\mathbf{k}_1,\mathbf{k}_2) U_1(\mathbf{k}_2,\mathbf{k}_3), \tag{40}$$

which, as shown in Appendix D, may be reduced to a twofold integral that must be evaluated numerically. There are twelve diagrams of this kind. When we ex-

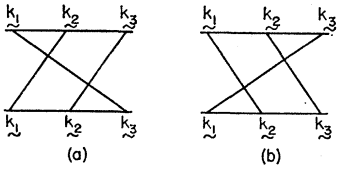

FIG. 1. Diagram representation of the $U_1U_1U_1$ terms arising in the calculation of U_3^s.

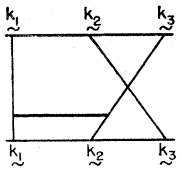

FIG. 2. Diagram representation of a typical U_1U_2 term arising in the calculation of U_3^s.

pand U_2 in spherical harmonics, we find that for even l's their contributions are identical and add, while for odd l's they are identical in magnitude, but not in sign, and give a zero total.

We next consider diagrams evolving from the expansion of U_3 in terms of binary kernels U_2 and X. The general matrix element of U_3, $\langle \mathbf{k}_1,\mathbf{k}_2,\mathbf{k}_3|\,U_3\,|\,\mathbf{k}_1,\mathbf{k}_2,\mathbf{k}_3\rangle$, gives us the six diagrams shown in Fig. 3, which exhaust the terms having only two binary kernels. To obtain $\langle \mathbf{k}_1,\mathbf{k}_2,\mathbf{k}_3|\,U_3^s\,|\,\mathbf{k}_1,\mathbf{k}_2,\mathbf{k}_3\rangle$ we must, then, consider these six diagrams for $\mathbf{k}_1'$, $\mathbf{k}_2'$, $\mathbf{k}_3'$ equal in turn to each of the six permutations of $\mathbf{k}_1$, $\mathbf{k}_2$, $\mathbf{k}_3$. This will give us 36 diagrams. However, we can take advantage of the fact that we are only interested in the integral over $\mathbf{k}_1$, $\mathbf{k}_2$, and $\mathbf{k}_3$ of $\langle \mathbf{k}_1,\mathbf{k}_2,\mathbf{k}_3|\,U_3^s\,|\,\mathbf{k}_1,\mathbf{k}_2,\mathbf{k}_3\rangle$. This will enable us to express our answer b_3^s in terms of only two diagrams.

Take any diagram, such as that illustrated in Fig. 4(a). There exists a permutation P such that this diagram may be re-expressed as a standard diagram, Fig. 4(b), where

$$\bar{k}_i = k_{PP'P^{-1}i}, \quad k_i' = k_{P'i}. \tag{41}$$

Instead of being formal about this, let us look at the example shown in Fig. 5. The equality obtains trivially as we have not changed at all the expression represented by the diagram. To obtain the second step we consider the $\mathbf{k}$'s as dummy variables and in this particular example apply a permutation P: (1,2,3) → (2,1,3) to their indices.

We may apply the same procedure to all the diagrams differing in appearance from our standard diagram. The mapping $P' \to PP'P^{-1}$ is an inner automorphism: it is one-to-one and isomorphic. This means

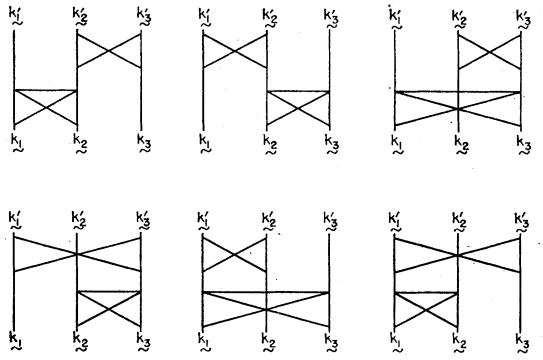

FIG. 3. Diagram representation of the terms involving two binary kernels which arise in the binary expansion of U_3.

that any "nonstandard" diagram, and the six permutations P' associated with it, may be replaced by the standard diagram where $\mathbf{k}_1'$, $\mathbf{k}_2'$, and $\mathbf{k}_3'$ are in turn set equal to the six permutations of $\mathbf{k}_1$, $\mathbf{k}_2$, and $\mathbf{k}_3$. The problem has, therefore, been reduced to considering the standard diagram and six different sets of $\mathbf{k}$'s. A weight of six will be associated with each case.

When we write down the expression for the standard diagram, taking advantage of the δ functions inherent in U_1, U_2, and X, as well as of the possibility of exchanging dummy variables, we find that we may represent the cases associated with the four P': (1,2,3) → [(1,2,3); (1,3,2); (2,1,3); (2,3,1)] by one single diagram belonging to the identity permutation, subject only to the restrictions that in the expansion of U_2 and X in spherical harmonics we restrict ourselves to even values of l and l'. We refer to this diagram as II, shown in

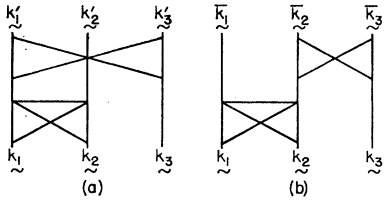

FIG. 4. A typical diagram (a) with primed variables re-expressed as a standard diagram, (b) with barred variables.

Fig. 6(b). It will have a weight of 24. The other two permutations P': (1,2,3) → [(3,1,2); (3,2,1)] may be represented by one of them, subject to the restrictions that in the expansion of U_2, we let l assume only even values. We shall then see, upon evaluating the diagram further, that this will imply that the odd values of l', belonging to X, will not contribute. We refer to this diagram as I, shown in Fig. 6(a). It will have a weight of 12.

The contribution to $\langle \mathbf{k}_1',\mathbf{k}_2',\mathbf{k}_3'|\,U_3\,|\,\mathbf{k}_1,\mathbf{k}_2,\mathbf{k}_3\rangle$ from a standard diagram reads

$$\int d\beta' \left\{ \int d^9k'' [U_1(\mathbf{k}_1',\mathbf{k}_1'')U_2(\mathbf{k}_2',\mathbf{k}_3';\,\mathbf{k}_2'',\mathbf{k}_3'')]_{\beta'} \times [X(\mathbf{k}_1'',\mathbf{k}_2'';\,\mathbf{k}_1,\mathbf{k}_2)U_1(\mathbf{k}_3'';\,\mathbf{k}_3)]_{\beta-\beta'} \right\}. \tag{42}$$

If we take advantage of the fact that

$$U_1(\mathbf{k}_1',\mathbf{k}_1'') = \delta(\mathbf{k}_1'-\mathbf{k}_1'') \exp(-\hbar^2\beta k_1'^2/2m)$$

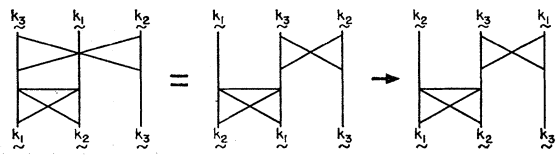

FIG. 5. A specific example of the reduction of a diagram to another in standard form.

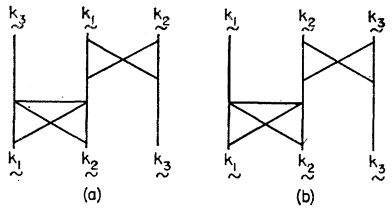

FIG. 6. Diagram representation of the two terms arising in the binary expansion of U_3^s to which all terms involving two binary kernels reduce.

and that U_2 and X are of the form:

$$U_2(\mathbf{k}_2',\mathbf{k}_3';\mathbf{k}_2'',\mathbf{k}_3'') = \delta(\mathbf{k}_2'+\mathbf{k}_3'-\mathbf{k}_2''-\mathbf{k}_3'')\mathfrak{U}_2(\mathbf{k}_2',\mathbf{k}_3';\mathbf{k}_2'',\mathbf{k}_3''),$$
$$X(\mathbf{k}_1'',\mathbf{k}_2'';\mathbf{k}_1,\mathbf{k}_2) = \delta(\mathbf{k}_1''+\mathbf{k}_2''-\mathbf{k}_1-\mathbf{k}_2)\mathfrak{X}(\mathbf{k}_1'',\mathbf{k}_2'';\mathbf{k}_1,\mathbf{k}_2), \quad (43)$$

we, then, can write Eq. (42) as

$$\delta(\sum_i \mathbf{k}_i'-\sum_i \mathbf{k}_i)\int_0^\beta d\beta' \times\exp(-\hbar^2\beta' k_1''^2/2m)\mathfrak{U}_2(\mathbf{k}_2',\mathbf{k}_3';\mathbf{k}_2'',\mathbf{k}_3)_{\beta'} \times\mathfrak{X}(\mathbf{k}_1',\mathbf{k}_2'';\mathbf{k}_1,\mathbf{k}_2)_{\beta-\beta'}\exp[-\hbar^2(\beta-\beta')k_3^2/2m], \quad (44)$$

where

$$\mathbf{k}_2''=\mathbf{k}_2'+\mathbf{k}_3'-\mathbf{k}_3.$$

We always choose the primed variables to be a permutation of the unprimed ones, and hence the delta function has a zero argument. It is evaluated as $\Omega/8\pi^3$. Equation (44) is the basis of a detailed evaluation, given in Appendix D, which result in expressions involving four-dimensional integrals which must be evaluated numerically.

The diagrams involving three kernels can easily be written. As in the previous case it is only necessary to calculate the two diagrams shown in Fig. 7, having weights 24 and 48. The integrals associated with these diagrams are at least six-dimensional and we shall not attempt to evaluate them.

RESULTS

The expressions given in Appendix D were the object of programs we wrote for the IBM 704 and 7090 of the AEC Computing Center at New York University. Resulting values for the third virial coefficients, compared with experimental data, are found in Table II.

We see that C_{theor} increases as the temperature decreases and remains positive throughout the range of temperatures that we considered.[20] The experimental data behave quite differently and decrease with decreasing temperature. They become negative around 4° K. In addition, the data of Keesom indicate a sharp drop in the value of the virial near 2° K.

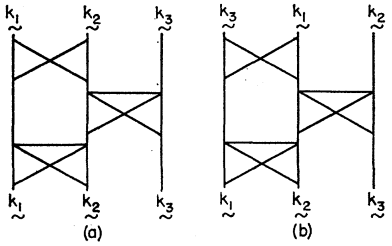

FIG. 7. Diagram representation of the two terms arising in the binary expansion of U_3^s to which all terms involving three binary kernels reduce.

TABLE II. Theoretical values, for the third virial coefficient, contrasted with experimental data. The C's are expressed in units of cc²/mole².

T (°K)	C_{exp} Keesom[a,b]	Keller[c]	K&W, re-ev.[d]	C_{theor} Bin. coll.	Bin. coll. & bound state
1.7	$-2.5\ 10^5$			$1.8\ 10^5$	$-2.2\ 10^5$
2.154		$-5.231\ 10^3$			
2.324		$-3.855\ 10^3$			
2.61	$-2.4\ 10^4$		$-1.8\ 10^4$		
2.862		$-7.282\ 10^3$			
3.105	$-5.28\ 10^3$		$-4.361\ 10^3$		
3.348		$-8.23\ 10^2$			
3.721	$-7.79\ 10^2$		$-1.747\ 10^3$		
3.961		$-3.58\ 10^2$			
4.0	$-3.0\ 10^2$			$3.5\ 10^4$	$7.5\ 10^3$
4.245	$-1.31\ 10^2$		$1.013\ 10^3$		
6.0	$4.6\ 10^2$				
8.0	$5.1\ 10^2$			$1.0\ 10^4$	$5.8\ 10^3$

[a] The value of 1.7° K is part of a set of values determined by Kistemaker and Keesom through extrapolation of the data of Keesom and Walstra. These values are found to be in rather good agreement with the direct evaluation of the C's, when the B's were extrapolated. The values for $T=4$, 6, and 8° K are taken from the table of "adopted values" from Keesom's *Helium*, and represent smoothed and interpolated values. We note from Fig. 6, page 36, of this book that there exists no direct measurements of C from about 4.25 to about 14 or 15° K. C changes very much in this region, however, and our values for 6 and 8° K, therefore, represent educated guesses at best. We have also included values for the isotherms of Keesom and Walstra which have been reanalyzed by Keller.

[b] J. Kistemaker and W. H. Keesom, Physica **12**, 227 (1946); W. H. Keesom, *Helium* (Elsevier Press, Amsterdam, Holland, 1942); W. H. Keesom and W. K. Walstra, Physica **7**, 985 (1940).

[c] W. E. Keller, Phys. Rev. **97**, 1 (1955).

[d] Keller, in the above reference, re-evaluates the data of Keesom and Walstra and obtains the values found in this column.

To reconcile these results would require large changes in b_3^s. While we expect inaccuracies in C_{theor} stemming from the use of only the leading terms in the binary expansion, and while we suspect that C_{theor} is sensitive to the shape of the potential, these factors would not be expected to be of such a magnitude as to account for this great disparity. This, as well as the sharp drop in the experimental value reported by Keesom, suggests that a physical property of helium has been overlooked.

In the next section we show that the inclusion of a three-body bound state will allow us to understand the experimental results at low temperatures. Further, we shall see that this procedure is supported by an approximate calculation which shows that such a state exists for our binary potential.

THREE-BODY BOUND STATE

To estimate the contribution of a three-body bound state we follow a method originated by Pais and

[20] We note that in their weak binding limit which is characterized by the presence of zero energy, virtual or real, two- and three-body bound states, Pais and Uhlenbeck obtain an expression for the third virial which is large and positive below 1° K.

Uhlenbeck[8] and we approximate the physical situation to that of two independent gases, helium atoms and triatomic molecules, in mutual equilibrium. The true grand partition function then reduces to the product of grand partition functions and its logarithm to the sum of logarithms. Using indices 1 and 3 to signify atoms and molecules, respectively, we then obtain

$$\ln Q^{(1)}+\ln Q^{(3)} = V\sum_l b_l^{(1)} z_{(1)}{}^l + V\sum_l b_l^{(3)} (e^{\beta\epsilon_3})^l z_{(3)}{}^l, \quad (45)$$

where $b_l^{(1)}$ and $b_l^{(3)}$ are the fugacity coefficients of the gases considered separately, $z_{(1)}$ and $z_{(3)}$ their respective fugacities. The $(e^{\beta\epsilon_3})^l$ term arises in $Q^{(3)}$, as the energies of the possible l molecule states must include l times the binding energy of the molecule, and is carried over in the fugacity expansion.

If we now examine term by term the correct grand partition function, having fugacity z, and the approximate one, we see that we must set

$$z_{(1)}=z, \quad z_{(3)}=z^3. \quad (46)$$

The coefficient of z^3 in the fugacity expansion is, then, aside from the common factor V,

$$b_3{}^s = b_3{}^{(1)} + b_1{}^{(3)} e^{\beta\epsilon_3}, \quad (47)$$

and as[21]

$$b_1{}^{(3)} = \left(\frac{2\pi(3m)kT}{h^2}\right)^{3/2} = 3^{3/2}\lambda_T{}^{-3} \quad (48)$$

we write

$$b_3{}^s\lambda_T{}^3 = (b_3{}^s)_{\text{cont}}\lambda_T{}^3 + 3^{3/2}e^{\beta\epsilon_3}. \quad (49)$$

Similar results have been obtained by Pais and Uhlenbeck.

Our next step is to form an estimate of the binding energy of the three-body bound state. We do this by considering the case of an attractive square well identical, in width and depth, to the attractive part of the potential used previously. This dropping of the core eases our labor prodigiously and is probably not too drastic an approximation for the estimate we seek.

We, then, proceed with a variational calculation, using a trial wave function of a type first used by Feenberg[22] for the study of the triton:

$$\psi = e^{-K(r_{12}+r_{13}+r_{23})}. \quad (50)$$

We obtain

$$\bar{H} = -3V_0\left[1-e^{-2x}\left(\frac{4}{21}x^4+\frac{20}{21}x^3+2x^2+2x+1\right)\right] + \frac{15}{14}\left(\frac{\hbar^2}{ma^2}\right)x^2, \quad (51)$$

where

$$x=Ka, \quad V=-V_0 \text{ for a radius} \leq a.$$

Inserting the appropriate constants and minimizing $\bar{H}$ by varying x, we find that we have a bound state with a binding energy of 0.26° K.

We now use this value[23] for ϵ_3 and regard our former binary collisions result as representing the continuum part of $b_3{}^s$. In Table II we show the resulting values for C_{theor}, which may again be contrasted with experimental values.

C_{theor} now reproduces the most obvious qualitative feature of the experimental third virial in that it is now negative at 1.7° K and positive for our higher temperatures. Since this behavior represents the most important information to be deduced from the experimental data, the exact experimental values being most uncertain, we conclude that our new results are in agreement with experiment.

Further, we take these results, together with the variational calculation, as support for a proposal that He^4 has a three-body bound state.

ACKNOWLEDGMENTS

I wish to express my appreciation to Professor T. D. Lee for suggesting this problem and I am much indebted to him for his guidance and very valuable suggestions and advice.

I should like to thank Dr. F. Mohling for his helpful conversations during his stay at Columbia. Also, thanks are due to the staffs of the Nevis Cyclotron Laboratory of Columbia University, the AEC Computing Center of New York University and the National Bureau of Standards for their aid and hospitality. I am grateful for the Pfister Fellowships and AEC support during the time of this work.

APPENDIX A: FITTING TO SECOND VIRIAL DATA

In determining the value of σ we take advantage of the fact that the leading contribution of the virial at high temperatures comes from the repulsive core. Further, we find that when the parameters n and s are allowed to vary within the broad range that we shall consider when fitting at low temperatures, the classical virial at high temperatures do not vary appreciably. For example, if we evaluate the virial for $n=1, 3, 4$, $s=0.99$, $\sigma=2.1$, we find that it differs by less than 1% from the value of the virial for $n=2$. If we allow s to change to $s=0.95$ our results are similar. The high-temperature virial, then, is a function of σ only, within the range of parameters that we consider; and we find that $\sigma=2.1$ Å. This value is well determined since for $\sigma=2.0$ Å every theoretical virial is smaller than every experimental virial (for the range 375–575° K) and for $\sigma=2.2$ Å the converse is true. Further, even if we drag all the experimental results down by 0.5 or increase them by 0.5, than $\sigma=2.0$ Å would still be too low and $\sigma=2.2$ Å would still be too high.

At low temperature we fit the second virial coefficient

[21] Rotational or vibrational energy levels, ϵ_t, in the triatomic molecule would have the effect of letting $b_1{}^{(3)} \to 3^{3/2}\lambda_T{}^{-3}\sum_t g_t e^{-\beta\epsilon_t}$.

[22] E. Feenberg, Phys. Rev. 47, 850 (1935).

[23] If we determine ϵ_3 by requiring that the addition of the bound state bring perfect agreement with the data of Kistemaker and Keesom at 1.7° K, then $\epsilon_3=0.4$° K.

to the experimental data over the range 1.7 to 8.2° K. These bounds stem on the one hand from the lack of reasonably accurate experimental information at lower temperatures, and on the other hand from the need for large number of angular momenta to evaluate accurately the second virial at high temperatures. Already, at our highest temperatures this factor limits our accuracy to not much better than 1%, although we use phase shifts of angular momenta $l=0, 2, 4, 6, 8, 10$.

APPENDIX B: EVALUATION OF THE A MATRIX

Given a 2-body potential of the following form

$$\begin{aligned} V(r)&=U \quad \text{for} \quad 0<r<\sigma \\ &=-\epsilon \quad \text{for} \quad \sigma<r<a \\ &=0 \quad \text{for} \quad a<r, \end{aligned}$$

where U is very large compared to ϵ, we wish to determine the appropriate radial wave functions for the case $y^2<(m/\hbar^2)U$. Corresponding to the three different regions, we have

$$\begin{aligned} \Phi_1&=\mathfrak{A} j_l(i\beta r), \\ \Phi_2&=\mathfrak{B} j_l(\kappa r)+\mathfrak{C}\eta_l(\kappa r), \\ \Phi_3&=y[\cos\delta_l j_l(yr)-\sin\delta_l \eta_l(yr)], \end{aligned} \tag{52}$$

where

$$\begin{aligned} \beta&=(mU/\hbar^2-y^2)^{1/2}, \\ \kappa&=(m\epsilon/\hbar^2+y^2)^{1/2}. \end{aligned}$$

This expression for Φ_3 insures that

$$\Phi_3 \longrightarrow r^{-1}\sin(yr-l\pi/2+\delta_l)$$

as r becomes large. The j's and η's are spherical Bessel and Neumann functions, respectively. In terms of ordinary Bessel functions, they may be written a

$$\begin{aligned} j_l(\rho)&=(\pi/2\rho)^{1/2}J_{l+\frac{1}{2}}(\rho), \\ \eta_l(\rho)&=-(-1)^l(\pi/2\rho)^{1/2}J_{-(l+\frac{1}{2})}(\rho). \end{aligned} \tag{53}$$

We recall our previous definition of the A matrix

$$\begin{aligned} \langle k|A_l|y\rangle&=-k^{-1}(m/\hbar^2)\int_0^\infty dr\, F_l(kr)V(r)\phi_y{}^l(r) \\ &=-(m/\hbar^2)\int_0^\infty dr\, r^2 j_l(kr)V(r)\Phi[\cos\delta_l(y)]^{-1} \\ &=(m/\hbar^2)[\cos\delta_l(y)]^{-1}(\mathrm{I}+\mathrm{II}+\mathrm{III}), \end{aligned} \tag{54}$$

where

$$\begin{aligned} \mathrm{I}&=U(\beta^2+k^2)^{-1}\mathfrak{A}\{r^2[i\beta j_l(kr)j_{l+1}(i\beta r) \\ &\qquad -kj_{l+1}(kr)j_l(i\beta r)]\}\,|_0{}^\sigma, \\ \mathrm{II}&=\epsilon(\kappa^2-k^2)^{-1} \\ &\quad\times\mathfrak{B}\{r^2[\kappa j_l(kr)j_{l+1}(\kappa r)-kj_{l+1}(kr)j_l(\kappa r)]\}\,|_\sigma{}^a, \\ \mathrm{III}&=\epsilon(\kappa^2-k^2)^{-1} \\ &\quad\times\mathfrak{C}\{r^2[\kappa j_l(kr)\eta_{l+1}(\kappa r)-kj_{l+1}(kr)\eta_l(\kappa r)]\}\,|_\sigma{}^a, \end{aligned} \tag{55}$$

and we have used the following formula

$$\begin{aligned} &\int_a^b x^2 z_l(\alpha x)z_l(\beta x)dx \\ &\quad=\{x^2[\beta z_l(\alpha x)z_{l+1}(\beta x)-\alpha z_{l+1}(\alpha x)z_l(\beta x)]\}\,|_a{}^b \\ &\qquad\times(\beta^2-\alpha^2)^{-1}. \end{aligned} \tag{56}$$

We have let z stand for any linear combination of j_l and η_l with real or imaginary coefficients.

If we evaluate $\mathfrak{A}$, $\mathfrak{B}$, $\mathfrak{C}$ by using the boundary conditions on the wave functions, we find that

$$\begin{aligned} \mathfrak{A}&=\mathfrak{B}(\kappa\sigma^2\bar{\Delta}_l)^{-1}, \\ \mathfrak{B}&=\bar{\Delta}_l y\cos\delta_l(y)[j_l(ya)-\tan\delta_l(y)\eta_l(ya)] \\ &\qquad\times[\bar{\Delta}_l j_l(\kappa a)-\bar{\Gamma}_l\eta_l(\kappa a)]^{-1}, \\ \mathfrak{C}&=-\mathfrak{B}\bar{\Gamma}_l(\bar{\Delta}_l)^{-1}, \end{aligned} \tag{57}$$

where $\bar{\Delta}$ and $\bar{\Gamma}$ are defined by

$$\begin{aligned} (2l+1)\bar{\Delta}_l&=j_l(i\beta\sigma)\kappa[l\eta_{l-1}(\kappa\sigma)-(l+1)\eta_{l+1}(\kappa\sigma)] \\ &\quad-\eta_l(\kappa\sigma)(i\beta)[lj_{l-1}(i\beta\sigma)-(l+1)j_{l+1}(i\beta\sigma)], \\ (2l+1)\bar{\Gamma}_l&=j_l(i\beta\sigma)\kappa[lj_{l-1}(\kappa\sigma)-(l+1)j_{l+1}(\kappa\sigma)] \\ &\quad-j_l(\kappa\sigma)(i\beta)[lj_{l-1}(i\beta\sigma)-(l+1)j_{l+1}(i\beta\sigma)]. \end{aligned} \tag{58}$$

We do not write the A matrix in terms of these expressions already at our disposal as it would not then be written in terms of real quantities only. Rather, if we look at the trigonometric representation of the spherical Bessel function, we will observe that if we let

$$j_l(ix)=(-i)^l\phi_l(x), \tag{59}$$

then ϕ_l will be real for all l, whenever x is also real. The introduction of such ϕ's results in a definitive expression for the A matrix in which all the terms are real.

$$\begin{aligned} \langle k|A_l|y\rangle&=y[j_l(ya)-\tan\delta_l(y)\eta_l(ya)][\Delta_l j_l(\kappa a)-\Gamma_l\eta_l(\kappa a)]^{-1} \\ &\quad\times\{(mU/\hbar^2)[\beta j_l(k\sigma)\phi_{l+1}(\beta\sigma)-kj_{l+1}(k\sigma)\phi_l(\beta\sigma)][\kappa(\beta^2+k^2)]^{-1} \\ &\quad+(m\epsilon/\hbar^2)\Delta_l\{a^2[\kappa j_l(ka)j_{l+1}(\kappa a)-kj_{l+1}(ka)j_l(\kappa a)]-\sigma^2[\kappa j_l(k\sigma)j_{l+1}(\kappa\sigma)-kj_{l+1}(k\sigma)j_l(\kappa\sigma)]\}[\kappa^2-k^2]^{-1} \\ &\quad-(m\epsilon/\hbar^2)\Gamma_l\{a^2[\kappa j_l(ka)\eta_{l+1}(\kappa a)-kj_{l+1}(ka)\eta_l(\kappa a)] \\ &\qquad-\sigma^2[\kappa j_l(k\sigma)\eta_{l+1}(\kappa\sigma)-kj_{l+1}(k\sigma)\eta_l(\kappa\sigma)]\}[\kappa^2-k^2]^{-1}\}, \end{aligned} \tag{60}$$

where

$$\begin{aligned} &\beta=(mU/\hbar^2-y^2)^{1/2}, \quad \kappa=(m\epsilon/\hbar^2+y^2)^{1/2}, \quad y^2<mU/\hbar^2, \\ &(2l+1)\Gamma_l=\phi_l(\beta\sigma)\kappa[lj_{l-1}(\kappa\sigma)-(l+1)j_{l+1}(\kappa\sigma)]+j_l(\kappa\sigma)\beta[l\phi_{l-1}(\beta\sigma)+(l+1)\phi_{l+1}(\beta\sigma)], \\ &(2l+1)\Delta_l=\phi_l(\beta\sigma)\kappa[l\eta_{l-1}(\kappa\sigma)-(l+1)\eta_{l+1}(\kappa\sigma)]+\eta_l(\kappa\sigma)\beta[l\phi_{l-1}(\beta\sigma)+(l+1)\phi_{l+1}(\beta\sigma)]. \end{aligned} \tag{61}$$

We also require an expression for the tangent of the phase shifts, this is derived by imposing the boundary conditions

$$\Phi_2'(r)/\Phi_2(r)=\Phi_3'(r)/\Phi_3(r),$$

where $r=a$. We then easily obtain

$$\tan\delta_l(y)=\frac{[y/(2l+1)][lj_{l-1}(ya)-(l+1)j_{l+1}(ya)]-\gamma_l(y)j_l(ya)}{[y/(2l+1)][l\eta_{l-1}(ya)-(l+1)\eta_{l+1}(ya)]-\gamma_l(y)\eta_l(ya)}, \tag{62}$$

where

$$\gamma_l(y)=\frac{\kappa[\Delta_l/(2l+1)][lj_{l-1}(\kappa a)-(l+1)j_{l+1}(\kappa a)]-\kappa[\Gamma_l/(2l+1)][l\eta_{l-1}(\kappa a)-(l+1)\eta_{l+1}(\kappa a)]}{j_l(\kappa a)\Delta_l-\eta_l(\kappa a)\Gamma_l}, \tag{63}$$

$$\kappa=(m\epsilon/\hbar^2+y^2)^{1/2}.$$

APPENDIX C

The limit of the matrix elements of U_2 requires special mention. In evaluating the limit of

$$(k^2-k'^2)^{-1}\int_0^\infty dy\, f(k,k',y) \times[P(k^2-y^2)^{-1}-P(k'^2-y^2)^{-1}] \tag{64}$$

by l'Hospital's rule, we must be careful to recall that we may not with impunity commute the differential operator $\partial/\partial k$ and the P (principal) value. We must first go into the complex plane and evaluate the principal-value integral by considering it to be half of the sum of two integrals: one taken over a contour skirting the singularities from the top, the other skirting the singularities from the bottom. The limit will be given by

$$(2k)^{-1}\left(\frac{\partial}{\partial k}\int_0^\infty dy\, f(k,k',y)[(k^2-y^2)^{-1}-(k'^2-y^2)^{-1}]\right) =\int_0^\infty dy\, f(k,k,y)(k^2-y^2)^{-2}, \tag{65}$$

where both integrals must be understood to be evaluated in the manner specified above. Taking then advantage that in the same sense

$$f(k,k,k)\int_0^\infty dy\,[k^2-y^2]^{-2}=0, \tag{66}$$

we may, then, write our answer as

$$P\int dy\, L(y,k)(k^2-y^2)^{-1}, \tag{67}$$

where

$$L(y,k)\equiv[f(k,k,k)-f(k,k,y)][k^2-y^2]^{-1}$$

and where we have used the equivalence of an integral having a first-order singularity and the specified contour, and the P value of such an integral. We can now eliminate the need to take a principal value if, as has been done in the section on binary kernels, we subtract from the integral another principal-value integral which has a value of zero. We then obtain

$$-\int dy\,[L(k,k)-L(y,k)][k^2-y^2]^{-1},$$

where $L(k,k)$ is the limit of $L(y,k)$ as $y\to k$.

APPENDIX D

U_1U_2 Diagrams

We now evaluate the contribution to b_3^s of the U_1U_2 terms, a typical term being represented by the diagram of Fig. 2. There are twelve of these terms and they may be associated with the possible configurations of the diagram. The free line, representing U_1, may not be vertical, hence we have three positions available for its upper end point, and two positions for its lower end point, giving us six possibilities. Then, for each free-line configuration the interacting lines representing U_2 may or may not be crossed.

Suppose that we write the equation corresponding to the diagram drawn.

$$b_3^s=(\Omega 3!)^{-1}\int d^3k_1d^3k_2d^3k_3\, U_2(\mathbf{k}_1,\mathbf{k}_3;\mathbf{k}_1,\mathbf{k}_2)U_1(\mathbf{k}_2,\mathbf{k}_3) \tag{68}$$

$$=(\Omega 3!)^{-1}\int d^3k_1d^3k_2 \times U_2(\mathbf{k}_1,\mathbf{k}_2;\mathbf{k}_1,\mathbf{k}_2)\exp(-\beta\hbar^2k_2^2/2m).$$

We see that precisely half of our diagrams will look this way (modulo changes in dummy variables). The other half will give as a typical term

$$(\Omega 3!)^{-1}\int d^3k_1d^3k_2\, U_2(\mathbf{k}_2,\mathbf{k}_1;\mathbf{k}_1,\mathbf{k}_2)\exp(-\beta\hbar^2k_2^2/2m).$$

If we introduce variables $\mathbf{k}$ and $\mathbf{K}$, by

$$\mathbf{K}=(\mathbf{k}_1+\mathbf{k}_2),\quad \mathbf{k}=\tfrac{1}{2}(\mathbf{k}_1-\mathbf{k}_2),$$

then we may write

$$U_2(\mathbf{k}_1,\mathbf{k}_2;\mathbf{k}_1,\mathbf{k}_2)=U_2(\mathbf{k},\mathbf{K};\mathbf{k},\mathbf{K}),$$
$$U_2(\mathbf{k}_2,\mathbf{k}_1;\mathbf{k}_1,\mathbf{k}_2)=U_2(-\mathbf{k},\mathbf{K};\mathbf{k},\mathbf{K}). \tag{69}$$

Expanding in spherical harmonics we may then, in this case, write U_2 in the form

$$\Omega(2\pi)^{-3}\exp(-\beta K^2\hbar^2/4m)\sum_{l=0}^{\infty}(2l+1)\times P_l(\cos\Theta)f_l(\beta,k), \quad (70)$$

where, in terms of our former nomenclature, we have let $\mathbf{K}'=\mathbf{K}$ and $\mathbf{k}'=\pm\mathbf{k}$. $\cos\Theta$, which equals $\hat{k}\cdot\hat{k}'$, will then be ±1, respectively. The even Legendre polynomials will give us $+1$ for both terms, the odd polynomials will give us ±1, respectively. Hence, we see that the odd angular momenta will give us no contribution, while the terms add for the even angular momenta.

As $k_2^2=\frac{1}{4}(\mathbf{K}-2\mathbf{k})^2=\frac{1}{4}K^2+k^2-\mathbf{K}\cdot\mathbf{k}$, we may write

$$b_3{}^s=(2/\pi)\int dK\,K^2\int dk\,k^2\sum_{l=0,\text{ even}}^{\infty}(2l+1)f_l(\beta,k)\exp(-3\beta\hbar^2K^2/8m)\exp(-\beta\hbar^2k^2/2m)\int_{-1}^{+1}d\mu\exp(\beta\hbar^2Kk\mu/2m)$$

$$=(4/\pi)\beta^{-1}(2m/\hbar^2)\sum_{l=0,\text{ even}}^{\infty}(2l+1)\int dk\int dK\,K\exp(-3\beta\hbar^2K^2/8m)$$

$$\times\sinh(\beta\hbar^2Kk/2m)k\exp(-\beta\hbar^2k^2/2m)f_l(\beta,k), \quad (72)$$

where we have taken all 12 diagrams into account. Using

$$\int_0^{\infty}\exp(-AK^2)\sinh(BK)KdK=\exp(B^2/4A)(B/4A)(\pi/A)^{1/2}, \quad (73)$$

we shall then obtain

$$b_3{}^s=(64\pi)3^{-3/2}(\lambda_T{}^3)^{-1}\sum_{l=0,\text{ even}}^{\infty}(2l+1)\int_0^{\infty}dk\,k^2f_l(\beta,k)\exp(-\beta\hbar^2k^2/3m), \quad (74)$$

where

$$f_l(\beta,k)=(2\pi)^{-3}(A+B),$$

$$A=\lim_{p\to k}4\pi[kp(k^2-p^2)]^{-1}[\cos^2\delta_l(p)k\langle k|A_l|p\rangle\exp(-\hbar^2\beta p^2/m)-\cos^2\delta_l(k)p\langle p|A_l|k\rangle\exp(-\hbar^2\beta k^2/m)],$$

$$B=\lim_{p\to k}8(k^2-p^2)^{-1}\int_0^{\infty}dy\left[\frac{[f(k)\exp(-\hbar^2\beta k^2/m)-f(y)\exp(-\hbar^2\beta y^2/m)]}{k^2-y^2}\right.$$

$$\left.-\frac{[f(p)\exp(-\hbar^2\beta p^2/m)-f(y)\exp(-\hbar^2\beta y^2/m)]}{p^2-y^2}\right],$$

where

$$f(y)\equiv f(k,p,y)\equiv\langle k|A_l|y\rangle\langle p|A_l|y\rangle\cos^2\delta_l(y).$$

Off-Diagonal Diagrams

This diagram, illustrated in Fig. 6(a), contributes, with a weight of 12, to $b_3{}^s$.

$$b_{3,\mathrm{I}}{}^s=12(3!8\pi^3)^{-1}\int\int\int d^3k_1d^3k_2d^3k_3\int_0^{\beta}d\beta'\,\mathfrak{U}_2(\mathbf{k}_1,\mathbf{k}_2;\mathbf{k}_1+\mathbf{k}_2-\mathbf{k}_3,\mathbf{k}_3)_{\beta'}$$

$$\times\mathfrak{IC}(\mathbf{k}_3,\mathbf{k}_1+\mathbf{k}_2-\mathbf{k}_3;\mathbf{k}_1,\mathbf{k}_2)_{\beta-\beta'}\exp(-\hbar^2\beta k_3{}^2/2m). \quad (75)$$

Let

$$\mathbf{k}=\tfrac{1}{2}(\mathbf{k}_1-\mathbf{k}_2), \qquad \mathbf{k}_1=(\mathbf{k}+\tfrac{1}{2}\mathbf{K}),$$
$$\mathbf{k}'=\tfrac{1}{2}(\mathbf{k}_1+\mathbf{k}_2-2\mathbf{k}_3), \qquad \mathbf{k}_2=(-\mathbf{k}+\tfrac{1}{2}\mathbf{K}),$$
$$\mathbf{K}=\mathbf{k}_1+\mathbf{k}_2, \qquad \mathbf{k}_3=(-\mathbf{k}'+\tfrac{1}{2}\mathbf{K}).$$

We switch to these variables to take advantage of the form of our binary kernels. The Jacobian equals one.

$$b_{3,\mathrm{I}}{}^s=12(3!8\pi^3)^{-1}\int d^3kd^3k'd^3K\int_0^{\beta}d\beta'\exp[-\hbar^2\beta(k'^2+\tfrac{1}{4}K^2-\mathbf{k}'\cdot\mathbf{K})/2m]\mathfrak{U}_2(\mathbf{k},\mathbf{k}',\mathbf{K})_{\beta'}\mathfrak{IC}(-\mathbf{k}',\mathbf{k},\mathbf{K})_{\beta-\beta'}. \quad (76)$$

We interchange $\mathbf{k}$ and $\mathbf{k}'$ in $\mathfrak{U}_2$, taking advantage of this kernel's symmetry in the two arguments. Further, we factor the $\mathbf{K}$ dependence from $\mathfrak{U}_2$ and $\mathfrak{K}$ by defining

$$\mathfrak{U}_2(\mathbf{k}',\mathbf{k},\mathbf{K})_{\beta'}=\exp(-\beta'\hbar^2K^2/4m)\mathfrak{R}(\mathbf{k}',\mathbf{k})_{\beta'},$$
$$\mathfrak{K}(-\mathbf{k}',\mathbf{k},\mathbf{K})_{\beta-\beta'}=\exp[-(\beta-\beta')\hbar^2K^2/4m]\mathfrak{S}(-\mathbf{k}',\mathbf{k})_{\beta-\beta'}.$$

This enables us to write

$$b_{3,\mathrm{I}}{}^s=(12)(3!8\pi^3)^{-1}\int d^3K\exp[-\hbar^2\beta(-\mathbf{k}'\cdot\mathbf{K}+\tfrac{3}{4}K^2)/2m]$$
$$\times\int\int d^3kd^3k'\exp(-\hbar^2\beta k'^2/2m)\int_0^\beta d\beta'\,\mathfrak{R}(\mathbf{k}',\mathbf{k})_{\beta'}\mathfrak{S}(-\mathbf{k}',\mathbf{k})_{\beta-\beta'}. \quad (77)$$

Doing the $\mathbf{K}$ integral we obtain:

$$12(3!8\pi^3)^{-1}(8\pi m/3\hbar^2\beta)^{3/2}\int d^3k\int d^3k'\exp(-\hbar^2\beta k'^2/3m)\int_0^\beta d\beta'\,\mathfrak{R}(\mathbf{k}',\mathbf{k})_{\beta'}\mathfrak{S}(-\mathbf{k}',\mathbf{k})_{\beta-\beta'}. \quad (78)$$

We now expand $\mathfrak{R}$ and $\mathfrak{S}$:

$$\mathfrak{R}=\sum_{l=0}^{\infty}(2l+1)P_l(\cos\Theta)\mathfrak{R}_l,\qquad \mathfrak{S}=\sum_{l'=0}^{\infty}(2l'+1)P_{l'}(\cos\Theta)\mathfrak{S}_{l'},\quad \cos\Theta=\hat{k}\cdot\hat{k}'.$$

Consistent with our previous remarks on adding diagrams, we can only allow l to assume even values. We let l' range over all values.

$$\int d^3k\,\mathfrak{R}(\mathbf{k}',\mathbf{k})_{\beta'}\mathfrak{S}(-\mathbf{k}',\mathbf{k})_{\beta-\beta'}=2\pi\sum_{l=0,\text{ even}}^{\infty}\sum_{l'=0}^{\infty}(2l+1)(2l'+1)$$
$$\times(-1)^{l'}\int_0^\infty dk\,k^2\int_{-1}^{+1}d\mu\,P_l(\mu)P_{l'}(\mu)\mathfrak{R}_l(k',k)_{\beta'}\mathfrak{S}_{l'}(k',k)_{\beta-\beta'}$$
$$=2\pi\sum_{l=0,\text{ even}}^{\infty}2(2l+1)\int_0^\infty dk\,k^2\mathfrak{R}_l(k',k)_{\beta'}\mathfrak{S}_l(k',k)_{\beta-\beta'}. \quad (79)$$

We see that we obtain a contribution only for $l=l'$.

$$b_{3,\mathrm{I}}{}^s=(16\pi)^2 3^{-3/2}\lambda_T{}^{-3}\sum_{l=0,\text{ even}}^{\infty}(2l+1)\int_0^\infty dk\int_0^\infty dk'\,k^2k'^2\exp(-\hbar^2\beta k'^2/3m)\int_0^\beta d\beta'\,\mathfrak{R}_l(k',k)_{\beta'}\mathfrak{S}_l(k',k)_{\beta-\beta'}. \quad (80)$$

If we do the β integration analytically, we obtain, quite straightforwardly, the following expressions which will have to be treated numerically.

$$\lambda_T{}^3b_{3,\mathrm{I}}{}^s=(16\pi)^2 3^{-3/2}\sum_{l=0,\text{ even}}^{\infty}(2l+1)\int_0^\infty dk\int_0^\infty dk'\,k^2k'^2\exp(-\hbar^2\beta k'^2/3m)\mathfrak{F}, \quad (81)$$

where

$$\mathfrak{F}=\int_0^\beta d\beta'\,\mathfrak{R}_l(k',k)_{\beta'}\mathfrak{S}_l(k',k)_{\beta-\beta'}=(2\pi)^{-6}(\hbar^2/m)(\mathrm{I}+\mathrm{II}+\mathrm{III}+\mathrm{IV}+\mathrm{V}). \quad (82)$$

Let $\hbar^2/m=a$, then, we find the following expressions for I, II, III, IV, and V:

$$(\mathrm{I})=(4\pi/kk')^2(k^2-k'^2)^{-1}\cos^2\delta_l(k)k'\langle k'|A_l|k\rangle$$
$$\times\{\cos^2\delta_l(k')k\langle k|A_l|k'\rangle[a(k'^2-k^2)]^{-1}(e^{-a\beta k^2}-e^{-a\beta k'^2})-\cos^2\delta_l(k)k'\langle k'|A_l|k\rangle\beta e^{-a\beta k^2}\}, \quad (83)$$

$$(\mathrm{II})=8(4\pi/kk')(k^2-k'^2)^{-1}\cos^2\delta_l(k)k'\langle k'|A_l|k\rangle\int_0^\infty dy\left\{\left[\beta f(k)e^{-a\beta k^2}-f(y)\left(\frac{e^{-a\beta k^2}-e^{-a\beta y^2}}{a(y^2-k^2)}\right)\right](k^2-y^2)^{-1}\right.$$
$$\left.-\left[f(k')\left(\frac{e^{-a\beta k^2}-e^{-a\beta k'^2}}{a(k'^2-k^2)}\right)-f(y)\left(\frac{e^{-a\beta k^2}-e^{-a\beta y^2}}{a(y^2-k^2)}\right)\right](k'^2-y^2)^{-1}\right\}, \quad (84)$$

$$(\mathrm{III})=-8(4\pi/kk')(k^2-k'^2)^{-1}\cos^2\delta_l(k')k\langle k|A_l|k'\rangle$$
$$\times\int_0^\infty dz\left[f(k)\left(\frac{e^{-a\beta k^2}-e^{-a\beta k'^2}}{a(k'^2-k^2)}\right)-f(z)\left(\frac{e^{-a\beta z^2}-e^{-a\beta k'^2}}{a(k'^2-z^2)}\right)\right](k^2-z^2)^{-1}, \quad (85)$$

$$(\mathrm{IV})=8(4\pi/kk')(k^2-k'^2)\cos^2\delta_l(k)k'\langle k'|A_l|k\rangle\int_0^\infty dz\left[f(k)\beta e^{-\alpha\beta k^2}-f(z)\left(\frac{e^{-\alpha\beta z^2}-e^{-\alpha\beta k^2}}{a(k^2-z^2)}\right)\right](k^2-z^2)^{-1}. \tag{86}$$

Expressions III and IV should be calculated as a unit; and in fact, by changing variables from z to y, may be combined with expression II.

$$(\mathrm{V})=-64(k^2-k'^2)^{-1}\int_0^\infty dz\int_0^\infty dy\{\ \}, \tag{87}$$

where the bracket equals

$$\frac{f(k)}{k^2-z^2}\left[\frac{f(k)\beta e^{-\alpha\beta k^2}-f(y)[(e^{-\alpha\beta k^2}-e^{-\alpha\beta y^2})/a(y^2-k^2)]}{k^2-y^2}\right.$$
$$\left.-\frac{f(k')[(e^{-\alpha\beta k^2}-e^{-\alpha\beta k'^2})/a(k'^2-k^2)]-f(y)[(e^{-\alpha\beta k^2}-e^{-\alpha\beta y^2})/a(y^2-k^2)]}{k'^2-y^2}\right]$$
$$-\frac{f(z)}{k^2-z^2}\left[\frac{f(k)[(e^{-\alpha\beta z^2}-e^{-\alpha\beta k^2})/a(k^2-z^2)]-f(y)[(e^{-\alpha\beta z^2}-e^{-\alpha\beta y^2})/a(y^2-z^2)]}{k^2-y^2}\right.$$
$$\left.-\frac{f(k')[(e^{-\alpha\beta z^2}-e^{-\alpha\beta k'^2})/a(k'^2-z^2)]-f(y)[(e^{-\alpha\beta z^2}-e^{-\alpha\beta y^2})/a(y^2-z^2)]}{k'^2-y^2}\right].$$

Diagonal Diagram

This diagram, illustrated in Fig. 6(b), contributes, with a weight of 24, to $b_3{}^s$.

$$b_{3,\mathrm{II}}{}^s=24(3!8\pi^3)^{-1}\int\int\int d^3k_1d^3k_2d^3k_3\int_0^\beta d\beta'\exp(-\hbar^2\beta'k_1^2/2m)$$
$$\times\exp[-\hbar^2(\beta-\beta')k_3^2/2m]\mathfrak{U}_2(\mathbf{k}_2,\mathbf{k}_3;\mathbf{k}_2,\mathbf{k}_3)_{\beta'}\mathfrak{K}(\mathbf{k}_1,\mathbf{k}_2;\mathbf{k}_1,\mathbf{k}_2)_{\beta-\beta'}. \tag{88}$$

We introduce new variables $\mathbf{k}$, $\mathbf{k}'$, $\mathbf{K}$, $\mathbf{K}'$ and new functions $f(\beta,k)$ and $q(\beta,k')$ by:

$$\mathbf{k}=\tfrac{1}{2}(\mathbf{k}_2-\mathbf{k}_3),\quad \mathbf{k}_1=2\mathbf{k}'+\mathbf{k}+\mathbf{K}/2,$$
$$\mathbf{K}=\mathbf{k}_2+\mathbf{k}_3,\quad \mathbf{k}_2=\mathbf{k}+\mathbf{K}/2,$$
$$\mathbf{k}'=\tfrac{1}{2}(\mathbf{k}_1-\mathbf{k}_2),\quad \mathbf{k}_3=-\mathbf{k}+\mathbf{K}/2,$$
$$\mathbf{K}'=\mathbf{k}_1+\mathbf{k}_2,$$
$$f(\beta,k)=\exp(+\hbar^2\beta K^2/4m)\mathfrak{U}_2(\beta,K,k),$$
$$q(\beta,k')=\exp(+\hbar^2\beta K'^2/4m)\mathfrak{K}(\beta,K',k').$$

We shall take the independent variables to be $\mathbf{k}$, $\mathbf{k}'$, $\mathbf{K}$ and the Jacobian of the transformation will give us a factor of 8.

$$b_{3,\mathrm{II}}{}^s=(24)(3!8\pi^3)^{-1}8\int\int\int d^3Kd^3kd^3k'\exp\{-\hbar^2\beta[3k^2+2k'^2+(\mathbf{k}+2\mathbf{k}')\cdot\mathbf{K}+4(\mathbf{k}\cdot\mathbf{k}')+3K^2/4]/2m\}$$
$$\times\int_0^\beta d\beta'\exp[-\hbar^2\beta'(k'^2-k^2)/m]f(\beta',k)q(\beta-\beta',k'). \tag{89}$$

We can do the $\mathbf{K}$ integral, as well as the angular part of the $\mathbf{k}$ and $\mathbf{k}'$ integrals.

$$\int d^3K\exp\{-\hbar^2\beta[3K^2/4+(\mathbf{k}+2\mathbf{k}')\cdot\mathbf{K}]/2m\}=(8\pi m/3\hbar^2\beta)^{3/2}\exp[(\hbar^2\beta/6m)(4k'^2+4\mathbf{k}\cdot\mathbf{k}'+k^2)], \tag{90}$$

$$\int\int d^3kd^3k'\exp[-(\hbar^2\beta/3m)(4k^2+k'^2+4\mathbf{k}\cdot\mathbf{k}')]$$
$$=(4\pi)(2\pi)(3m/2\hbar^2\beta)\int_0^\infty dk\int_0^\infty dk'\,kk'\sinh(4\hbar^2\beta kk'/3m)\exp[-\hbar^2\beta(4k^2+k'^2)/3m]. \tag{91}$$

Expanding f and q:

$$f(\beta,k)=\sum_{l=0}^{\infty}(2l+1)f_l(\beta,k),\quad q(\beta,k')=\sum_{l'=0}^{\infty}(2l'+1)q_{l'}(\beta,k'),$$

and collecting all terms, we obtain

$$b_{2,\mathrm{II}}{}^{s}=(2\pi)^3(256)3^{-1/2}\lambda_T{}^{-5}\sum_{l,l'=0;\ \mathrm{even}}^{\infty}(2l+1)(2l'+1)$$
$$\times\int_0^\infty dk\int_0^\infty dk'\,kk'\sinh(4\hbar^2\beta kk'/3m)\exp[-\hbar^2\beta(4k^2+k'^2)/3m]$$
$$\times\int_0^\beta d\beta'\exp[-\hbar^2\beta'(k'^2-k^2)/m]f_l(\beta',k)q_{l'}(\beta-\beta',k'). \quad (92)$$

We sum only over the even angular momenta. Performing the β integration we have

$$\int_0^\beta d\beta'\exp[-\hbar^2\beta'(k'^2-k^2)/m]f_l(\beta',k)q_{l'}(\beta-\beta',k')=(2\pi)^{-6}(\hbar^2/m)\lim_{p\to k}(\mathrm{I}+\mathrm{II}+\mathrm{III}+\mathrm{IV}+\mathrm{V}), \quad (93)$$

where, if we again let $\hbar^2/m=a$,

$$(\mathrm{I})=\left(\frac{4\pi}{k'}\right)\cos^2\delta_{l'}(k')\tan\delta_{l'}(k')e^{-a\beta k'^2}\left(\frac{4\pi}{kp}\frac{1}{k^2-p^2}\right)$$
$$\times\left[\cos^2\delta_l(p)k\langle k|A_l|p\rangle\left(\frac{1-e^{-a\beta(p^2-k^2)}}{a(p^2-k^2)}\right)-\cos^2\delta_l(k)p\langle p|A_l|k\rangle\beta\right], \quad (94)$$

$$(\mathrm{II})=\left(\frac{4\pi}{k'}\right)\cos^2\delta_{l'}(k')\tan\delta_{l'}(k')e^{-a\beta k'^2}\left(\frac{8}{k^2-p^2}\right)\int_0^\infty dy\left[\frac{f_l(k)\beta-f_l(y)[(1-e^{-a\beta(y^2-k^2)})/a(y^2-k^2)]}{k^2-y^2}\right.$$
$$\left.-\frac{f_l(p)[(1-e^{-a\beta(p^2-k^2)})/a(p^2-k^2)]-f_l(y)[(1-e^{-a\beta(y^2-k^2)})/a(y^2-k^2)]}{p^2-y^2}\right], \quad (95)$$

where

$$f_l(y)\equiv f_l(k,p,y)\equiv\langle k|A_l|y\rangle\langle p|A_l|y\rangle\cos^2\delta_l(y).$$

$$(\mathrm{III})+(\mathrm{IV})=\frac{4\pi}{kp}\frac{1}{k^2-p^2}\cos^2\delta_l(p)k\langle k|A_l|p\rangle(-8)\int_0^\infty dz\left[\frac{e^{-a\beta k'^2}f_{l'}(k',k',k')[(1-e^{-a\beta(p^2-k^2)})/a(p^2-k^2)]}{k'^2-z^2}\right.$$
$$\left.-\frac{e^{-a\beta z^2}f_{l'}(k',k',z)[(1-e^{-a\beta(k'^2+p^2-k^2-z^2)})/a(k'^2+p^2-k^2-z^2)]}{k'^2-z^2}\right]+\frac{4\pi}{kp}\frac{1}{k^2-p^2}\cos^2\delta_l(k)p\langle p|A_l|k\rangle(8)$$
$$\times\int_0^\infty dz\,\frac{e^{-a\beta k'^2}f_{l'}(k',k',k')\beta-e^{-a\beta z^2}f_{l'}(k',k',z)[(1-e^{-a\beta(k'^2-z^2)})/a(k'^2-z^2)]}{k'^2-z^2}, \quad (96)$$

$$(\mathrm{V})=-8\left(\frac{8}{k^2-p^2}\right)\int_0^\infty dz\int_0^\infty dy\left\{\frac{f_{l'}(k',k',k')e^{-a\beta k'^2}}{k'^2-z^2}\left(\frac{f_l(k)\beta-f_l(y)[(1-e^{-a\beta(y^2-k^2)})/a(y^2-k^2)]}{k^2-y^2}\right.\right.$$
$$\left.-\frac{f_l(p)[(1-e^{-a\beta(p^2-k^2)})/a(p^2-k^2)]-f_l(y)[(1-e^{-a\beta(y^2-k^2)})/a(y^2-k^2)]}{p^2-y^2}\right)$$
$$-\frac{f_{l'}(k',k',z)e^{-a\beta z^2}}{k'^2-z^2}\left[\frac{f_l(k)[(1-e^{-a\beta(k'^2-z^2)})/a(k'^2-z^2)]-f_l(y)[(1-e^{-a\beta(k'^2+y^2-k^2-z^2)})/a(k'^2+y^2-k^2-z^2)]}{k^2-y^2}\right.$$
$$\left.\left.-\frac{f_l(p)[(1-e^{-a\beta(k'^2+p^2-k^2-z^2)})/a(k'^2+p^2-k^2-z^2)]-f_l(y)[(1-e^{-a\beta(k'^2+y^2-k^2-z^2)})/a(k'^2+y^2-k^2-z^2)]}{p^2-y^2}\right]\right\}. \quad (97)$$

APPENDIX E

TABLE III. The contributing terms to $b_3{}^s\lambda_T{}^3$.[a]

Temperature (°K)	1.7	4	8
Free	0.06415	0.06415	0.06415
2-dim.	0.6075	0.7444	0.6278
4-dim. off	0.3436	0.5808	0.8394
4-dim. dia.	−0.6809	−3.9531	−12.10
Total	0.3344	−2.564	−10.57

[a] It is estimated that the total results are accurate to within 2%, and that no contributing term has an error greater than 5%.

TABLE IV. A breakdown of the contributing terms to $b_3{}^s\lambda_T{}^3$ for 1.7° K.

$l=$		0	2	4	6	Total
Two-dimensional integrals		0.1804	0.4050	0.0216	0.0005	0.6075
Four-dimensional integrals (off-diagonal diagram)		0.2475	0.0940	0.0021	0.0000	0.3436
Four-dimensional integrals (diagonal diagrams)						−0.6809
l \ l'	0	2	4	6		
0	−0.2735	−0.3493	−0.0187	0.0000		
2	−0.0266	−0.0339	0.0051	0.0007		
4	0.0086	0.0058	−0.0005	0.0000		
6	0.0009	0.0007	0.0000	0.0000		

TABLE V. A breakdown of the contributing terms to $b_3{}^s\lambda_T{}^3$ for 4° K.

$l=$		0	2	4	6	Total
Two-dimensional integrals		−0.2810	0.7966	0.2075	0.0213	0.7444
Four-dimensional integrals (off-diagonal diagrams)		0.4009	0.1532	0.0267	0.0000	0.5808
Four-dimensional integrals (diagonal diagrams)						−3.9531
l \ l'	0	2	4	6		
0	−0.0995	−2.1147	−0.7129	−0.0957		
2	−0.6724	−0.0659	−0.0250	0.0000		
4	−0.1805	0.0226	0.0081	0.0000		
6	−0.0173	0.0000	0.0000	0.0000		

TABLE VI. A breakdown of the contributing terms to $b_3{}^s\lambda_T{}^3$ for 8° K.

$l=$		0	2	4	6	Total
Two-dimensional integrals		−0.7840	0.6517	0.5894	0.1707	0.6278
Four-dimensional integrals (off-diagonal diagram)		0.4833	0.2840	0.0588	0.0133	0.8394
Four-dimensional integrals (diagonal diagrams)						−12.10
l \ l'	0	2	4	6		
0	0.9625	−3.3824	−3.4167	−1.2074		
2	−0.9953	−1.0539	−0.9089	−0.4014		
4	−0.9466	−0.3403	−0.0067	−0.0005		
6	−0.3007	−0.1186	0.0111	0.0038		